UDC 624.920.427 : 534.014

SEISMIC DRIFT OF REINFORCED CONCRETE STRUCTURES

Technical Research Institute, K. Shimazaki
Professor of University of Illinois, M. A. Sozen

Key Words : Reinforced Concrete, Earthquake Response, Ground Motions, Nonlinear Systems, Response Spectra, Energy Spectra, Earthquake-Resistant Design, Single-degree-of-freedom System

Synopsis

Nonlinear displacement response of reinforced concrete structures is investigated by a parametric study of single-degree-of-freedom systems with appropriate hysteresis properties. Strength, stiffness, and the type of ground motion are the main variables considered. It is shown that a set of dimensionless parameters defining the three variables can be used to determine whether the displacement response can be satisfactorily determined using linear-response analysis.

1. INTRODUCTION

Distortion of a reinforced concrete structure caused by strong ground motion is an important factor in the planning and proportioning of reinforced concrete structural systems. This paper reports the results of a parametric study to investigate the effects of strength, stiffness, and type of ground motion on nonlinear displacement response. It is shown that nonlinear displacement response of analytical models with force-displacement properties similar to those of reinforced concrete under cyclic loads can be related simply and satisfactorily to linear-response spectral values using dimensionless parameters for strength, initial stiffness, and the type of ground motion.

Most of the generalizations about seismic response are based on Newmark's

observations of nearly constant response ranges of acceleration, velocity, and displacement, and how the magnitudes of these ranges can be modified on the basis of tolerable ductility limits. The tangible evidence for Newmark's initial observations on earthquake response rests in two studies[1),2)] of dynamic response using elasto-plastic models with equal and constant loading/unloading slopes. Recently, Otani[3)] re-evaluated the effect of differences in hysteresis models on response with results which generally confirmed Newmark's insights but indicated that for systems with periods less than 0.15 sec. the required ductility tended to be more than that anticipated.

In 1975, Kato and Akiyama[4)] returned to Housner's "energy input" concept[5)] for understanding structural damage. This work led to methods of design with energy as the basic principle[6)]. In an evaluation of structural response in relation to dissipated energy, Suzuki and Takeda[7)] noted that the nonlinear displacement response of a single-degree-of-freedom system should be treated differently in regions of constant-acceleration and constant-velocity response.

The work presented in this paper builds on ideas from the above sources to arrive at simple generalizations about the relationship of nonlinear to linear displacement response for reinforced concrete structures. Main parameters considered are ground-motion characteristics, hysteresis-model types, initial stiffness, and strength.

2. GROUND MOTION RECORDS

Three earthquake records were selected to represent the three general conditions of ground stiffness: hard, medium and soft.

The N21E horizontal component of the acceleration record obtained at Castaic, California during the 1971 San Fernando earthquake was considered to represent the type of motion to be encountered at a "hard" site. The N-S component of the record obtained at El Centro, California, during the 1940 Imperial Country Earthquake was assumed to represent the motion for a "medium" site. To represent the motion at a "soft" site, the E-W component of the record obtained at Hachinohe, Japan (Tokachi-Oki Earthquake 1968) was used. The Castaic 1971 N21E acceleration record was obtained from the U.S. Geological Survey, Menlo Park. The El Centro 1940 N-S and Hachinohe 1968 E-W acceleration records were obtained from the files at the Building Research Institute, Tsukuba, Japan.

After examination of various noise components in acceleration records, it was concluded by Trifunac et al.[8], that most of the noise in ground motion records was concentrated at the low- and high-frequency ends of the signals, and that a record filtered to eliminate a range of high and low frequencies would be a good representation of the true signal. To filter the three selected records in order to eliminate the effects attributed to spurious signals, the procedure proposed by Hodder[9] was selected, because it is simple to implement and because it has an adequate transition band width at the low-frequency end. Another positive attribute of Hodder's procedure is that its results are in very close agreement with those obtained by Sunder and Connor[10] who used a lengthier procedure.

The main features of the filter proposed by Hodder are shown in Fig. 1.

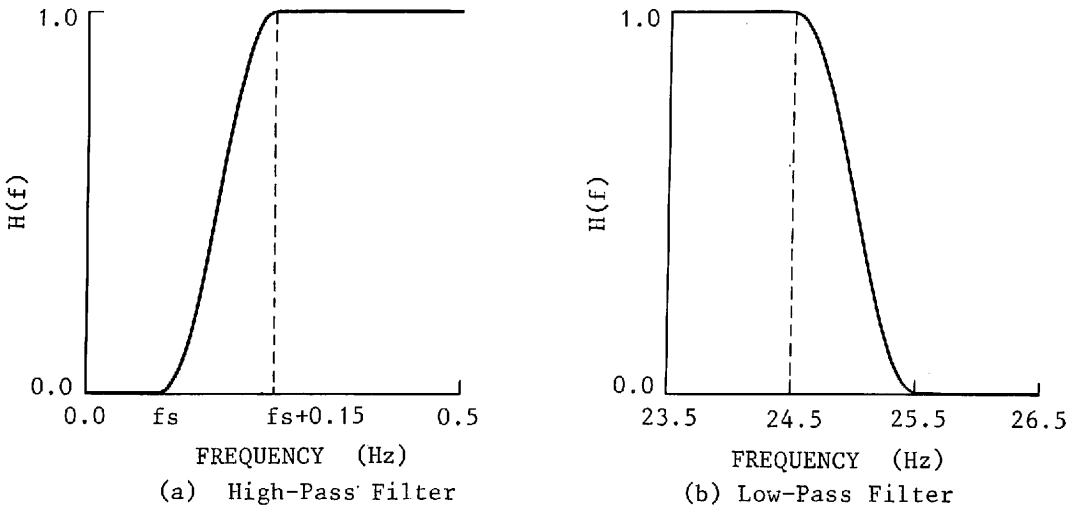

Fig. 1 Frequency Ranges for the Filter
(f_s = 0.1 Hz for El Centro and Hachinohe and 0.2 Hz for Castaic)

For the low-pass filter, rolloff starts at 24.5 Hz and stops at 25.5 Hz. Any component of the motion having a frequency higher than 25.5 is discarded. Between 24.5 and 25.5 Hz, signal components are multiplied by:

$$\sin^2\left[\frac{\pi}{2}\,\frac{25.5 - f}{25.5 - 24.5}\right] = \sin^2[\pi * (25.5 - f)/2.0] \qquad (1)$$

where, f is the frequency of the signal component considered.

Table 1. Ground Motion Records

	Acceleration		Velocity		Displacement		Filter[b]	
	Max. G	Time[a] sec.	Max. mm/sec.	Time sec.	Max. mm	Time sec.	High pass[c] Hz	Low pass[c] Hz
Castaic 1971 N21E	0.316 0.317	2.60 2.60	- 162.6	- 1.34	- 25.9	- 1.00	- 0.20	- 25.5
El Centro 1940 NS	0.349 0.348	2.14 2.14	- 336.0	- 2.18	- 71.6	- 5.08	- 0.10	- 25.5
Hachinohe 1968 EW	0.186 0.183	0.22 0.22	- 331.9	- 1.90	- 104.0	- 6.36	- 0.10	- 25.5

a) Time of occurrence of maximum value
b) After Hodder (Ref. 9)
c) Roll off termination frequency

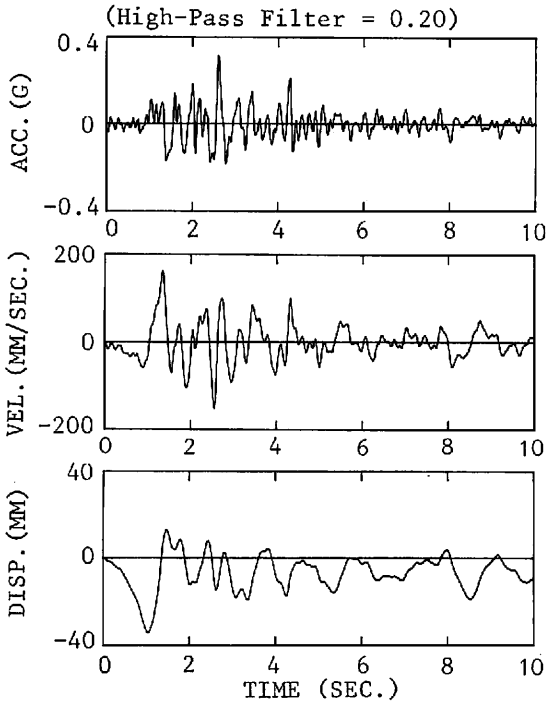

Fig. 2 Acceleration, Velocity and Displacement Histories for Castaic 1971 N21E

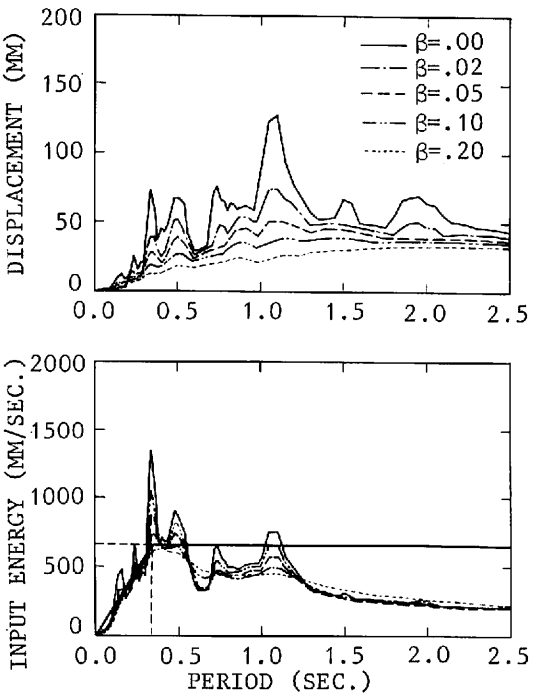

Fig. 5 Displacement and Energy Spectra (Castaic 1971 N21E)

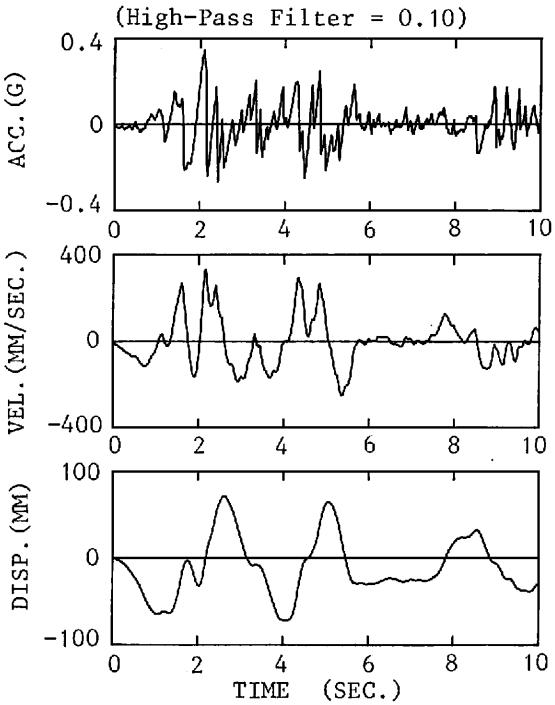

Fig. 3 Acceleration, Velocity and Displacement Histories for El Centro 1940 NS

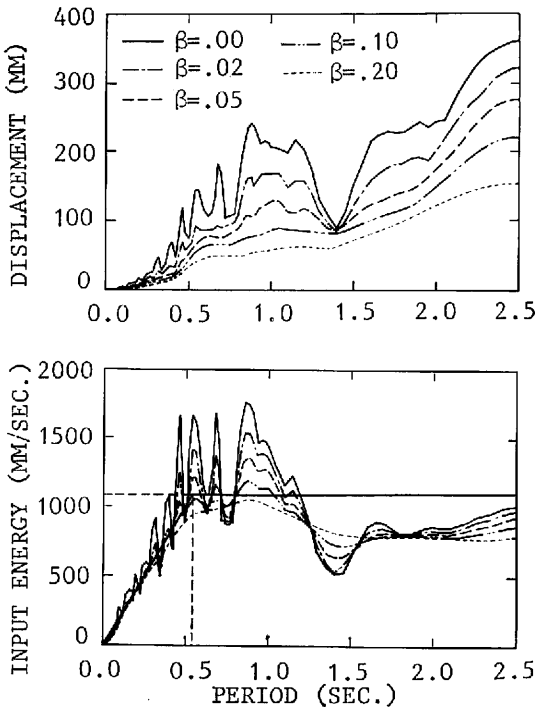

Fig. 6 Displacement and Energy Spectra (El Centro 1940 NS)

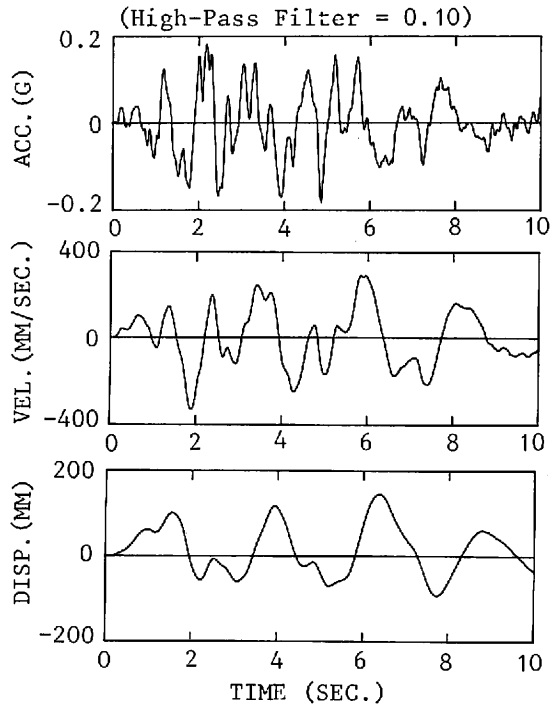

Fig. 4 Acceleration, Velocity and Displacement Histories for Hachinohe 1968 EW

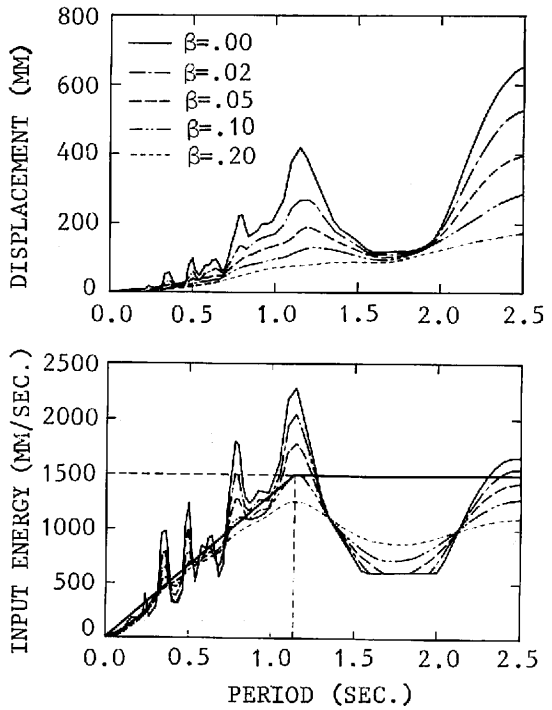

Fig. 7 Displacement and Energy Spectra (Hachinohe 1968 EW)

For the high-pass filter, rolloff starts at a frequency (f_s + 0.15) and ends at a frequency of f_s. The frequency f_s is the largest of 0.1 Hz, $3/T_L$, and $f_p/15$, where T_L is the duration of the record and f_p represents the frequency for the highest amplitude of the Fourier spectrum for the record.

In the 0.15-Hz range between the rolloff bounds, the signal component is multiplied by:

$$\sin^2[\frac{\pi}{2}\frac{f - f_s}{0.15}] = \sin^2[\pi * (f - f_s)/0.3] \qquad (2)$$

The two frequencies bounding the filter for the records processed are tabulated in the last column of Table 1. The filtered acceleration records and the computed velocity and displacement histories are shown in Fig. 2 through 4 for the first ten seconds. Table 1 shows the maximum acceleration values and the maximum computed velocity and displacement values as well as the time at which they occurred.

3. ENERGY RESPONSE SPECTRA

Displacement response and energy response spectra for the three ground motions are shown in Fig. 5 through 7. Response spectra were based on the first ten seconds of each acceleration record. Procedure for the determination of the energy response spectrum is described below.

The equation of motion of a linearly elastic SDOF system is:

$$m\ddot{x} + c\dot{x} + kx = -m\ddot{x}_g \qquad (3)$$

where, m : mass

c : coefficient of viscous damping

k : stiffness constant

x, $\dot{x}$, $\ddot{x}$: displacement, velocity, and acceleration of mass with

respect to base

$\ddot{x}_g$: acceleration of base

Equation (3) is written in terms of forces. It can also be written as a statement of energy balance during a very short time increment Δt.

$$m\ddot{x}(t) \cdot \Delta x + c\dot{x}(t) \cdot \Delta x + kx(t) \cdot \Delta x = - m\ddot{x}_g(t) \cdot \Delta x \tag{4}$$

To show the relation of Eq. (4) to familiar forms of energy, it may be integrated over a time period, t, recognizing that $\Delta x = \dot{x} \cdot \Delta t$ with Δt approaching zero,

$$m\int_0^t \ddot{x}\dot{x}dt + c\int_0^t \dot{x}^2 dt + k\int_0^t x\dot{x}dt = - m\int_0^t \ddot{x}_g\dot{x}dt \tag{5}$$

Integrating by parts,

$$\frac{m}{2}[\dot{x}(t)]^2 + \frac{k}{2}[x(t)]^2 + c\int_0^t \dot{x}^2 dt = - m\int_0^t \ddot{x}_g\dot{x}dt \tag{6}$$

The terms in Eq. (6) are interpreted as:

Kinetic Energy + Potential Energy + Dissipated Energy = Input Energy

To obtain the input energy for an oscillator of given stiffness and viscous damping, the left-hand side of Eq. (4) is evaluated numerically for calculated acceleration, velocity, and displacement responses over any specified part of a given ground-motion record. The maximum energy, E_m, determined during this process is the spectral value for the period and damping factor of the oscillator.

A convenient form for presenting energy response is the equivalent

velocity, V_e, obtained from Eq. (7).

$$V_e = \sqrt{\frac{E_m}{m}} \tag{7}$$

where E_m is maximum input energy and m is mass of the oscillator.

Akiyama[6] has suggested that the energy response spectrum can be represented ideally by two straight lines (Fig. 8) with the first line going through the origin and the second representing a "flat" bound. The period at the intersection of these two portions, TG, usually occurs at a value comparable to the period at the intersection of the constant-acceleration and constant-velocity response regions. In this paper, it will be called the characteristic period of the ground motion. The characteristic periods of the ground motions selected are indicated in Fig. 8.

	TG (sec.)	V_e (mm/sec.)
CASTAIC 1971 N21E	0.35	650
EL CENTRO 1940 NS	0.55	1100
HACHINOHE 1968 EW	1.20	1500

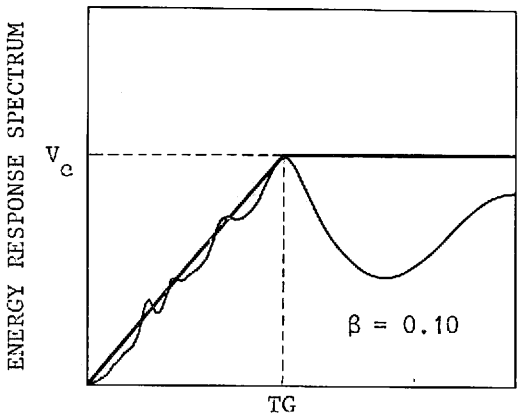

Fig. 8 Idealization of the Energy Response Spectrum

4. HYSTERESIS MODELS

The four hysteresis models used are illustrated in Fig. 9.

Hysteresis model 1 is the well-known elasto-plastic model with constant slope for loading and unloading. Even though it is a poor representation of the actual response for most structural engineering materials, it is useful because it represents a reasonable upper bound for energy dissipation.

Hysteresis model 2, used to represent reinforced concrete by Clough and Johnston[11], differs from model 1 because of changes in the stiffness of the loading slope.

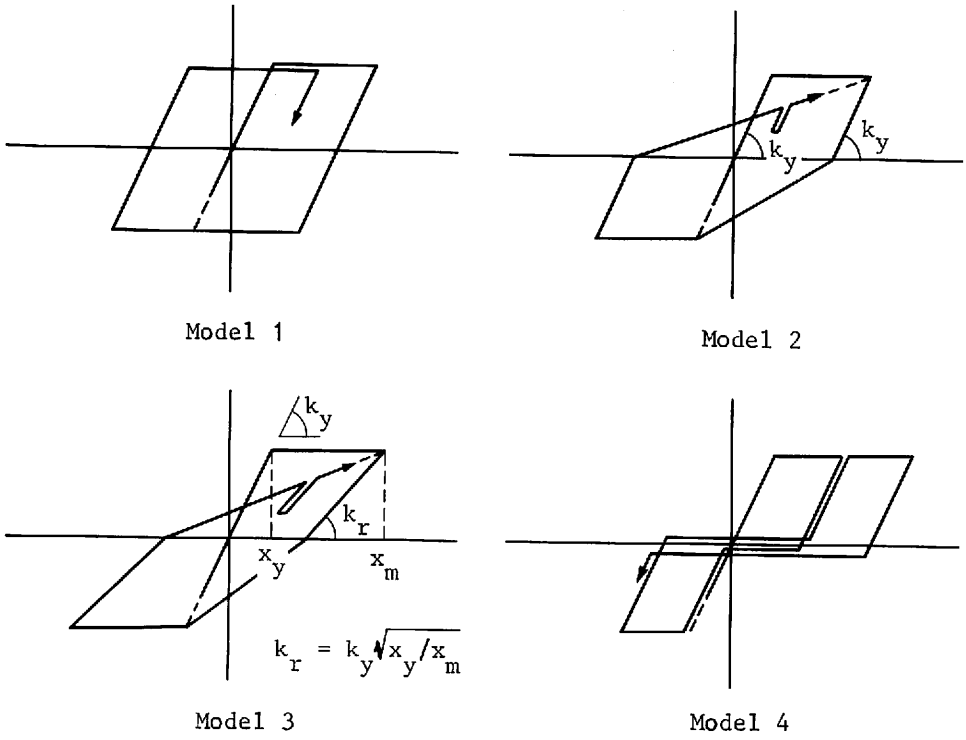

Fig. 9 Hysteresis Models

Hysteresis model 3, used by Otani[3] as a simplified version of the Takeda hysteresis[12] for reinforced concrete, is similar to model 2 except for the unloading slope which varies with loading history as indicated by Eq. (8).

$$K_r = K_y \left| \frac{x_m}{x_y} \right|^{-\alpha} \tag{8}$$

K_r : unloading stiffness

k_y : yielding stiffness

x_m : maximum displacement

x_y : yielding displacement

α : constant defining unloading stiffness

Hysteresis model 4 may be considered to be a variant of model 1. The main difference is the "slip"; loading in either direction does not start unless the point on the displacement axis corresponding to the immediately previous unloading is reached.

Relative energy dissipation capabilities of the first three models may be compared by using the equivalent viscous-damping values defined by Jacobsen[13].

For model 1, the equivalent viscous damping is given by Eq. (9).

$$\beta_1 = 2 * (1 - 1/\mu)/\pi \tag{9}$$

β_1 : equivalent viscous damping for hysteresis model 1

μ : ratio of maximum to yield displacement

For models 2 and 3,

$$\beta_2 = (1 - \mu^{(\alpha-1)})/\pi \tag{10}$$

β_2 : equivalent viscous damping for hysteresis models 2 and 3

Variations of the equivalent viscous-damping factors with the ductility ratio are compared in Fig. 10 for the first three models. The damping factors plotted refer to constant-amplitude cycles and are irrelevant to earthquake response, but they do provide a measure of the relative capabilities of the hysteresis systems to dissipate energy. Although a comparable value cannot be calculated directly for model 4, it is plausible to assume that model 4 has less energy-dissipation capability than the other three models.

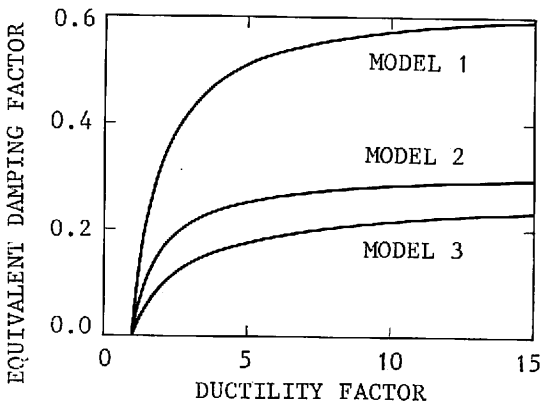

Fig. 10 Equivalent Damping Factor

5. CALCULATED DISPLACEMENT RESPONSE

To study the trends of calculated displacement response, calculations were made for a number of single-degree-of-freedom oscillators. The organization of the parametric studies is illustrated by the arrangement of Fig. 11. Two different initial stiffnesses were considered. Calculations for oscillators with an initial period of 0.3 are summarized in the top row of three plots and those for oscillators with an initial period of 1.0 sec. are summarized in the bottom row of three plots. Response was determined for the three ground motions attributed to hard, medium, and soft sites, leading to the six plots in Fig. 11. Each plot includes four curves, one for each of the hysteresis models discussed.

For each hysteresis model, calculations were made successively for a series of single-degree-of-freedom oscillators of increasing strength. If the response of an oscillator remained in the linear range, calculations were stopped for that series. The horizontal line in each figure represents the displacement corresponding to linear response.

Dynamic response was determined using Newmark's beta method[14] with beta set at 1/6. At instants of slope change of the assumed hysteresis, iterations were continued until both the equation of dynamic equilibrium and the overall hysteresis relationship were satisfied. Response was determined for a duration of ten seconds for each ground-motion record. Time interval was the smaller of 0.01 sec. and $T_0/20$, where T_0 is the initial period of the oscillator. The damping factor, which varied linearly with the stiffness, was assumed to have an initial value of 0.02.

The abscissas in Fig. 11 refer to the base shear strength coefficient, C_y, which defines the force at the initial break point (yielding) of the assumed force-displacement relationship as a ratio of the assumed weight of the oscillator. The ordinates are given in mm. Because of the low displacements calculated, the data for the Castaic record were poltted with a different y-axis scale.

For each combination of period and ground motion, the trends of the four curves obtained for different hysteresis models can be said to be generally similar. The curves for models 1-3 are more consistent with each other than with the curve for hysteresis model 4. The magnitudes of the response displacement for an oscillator of given strength are different for different hysteresis models. For the 0.3-sec. oscillator, the relative magnitudes of the displacement curves are in an order consistent with the equivalent damping implied by the hysteresis models, especially for the El Centro and Hachinohe motions. This result is attributed to the fact that

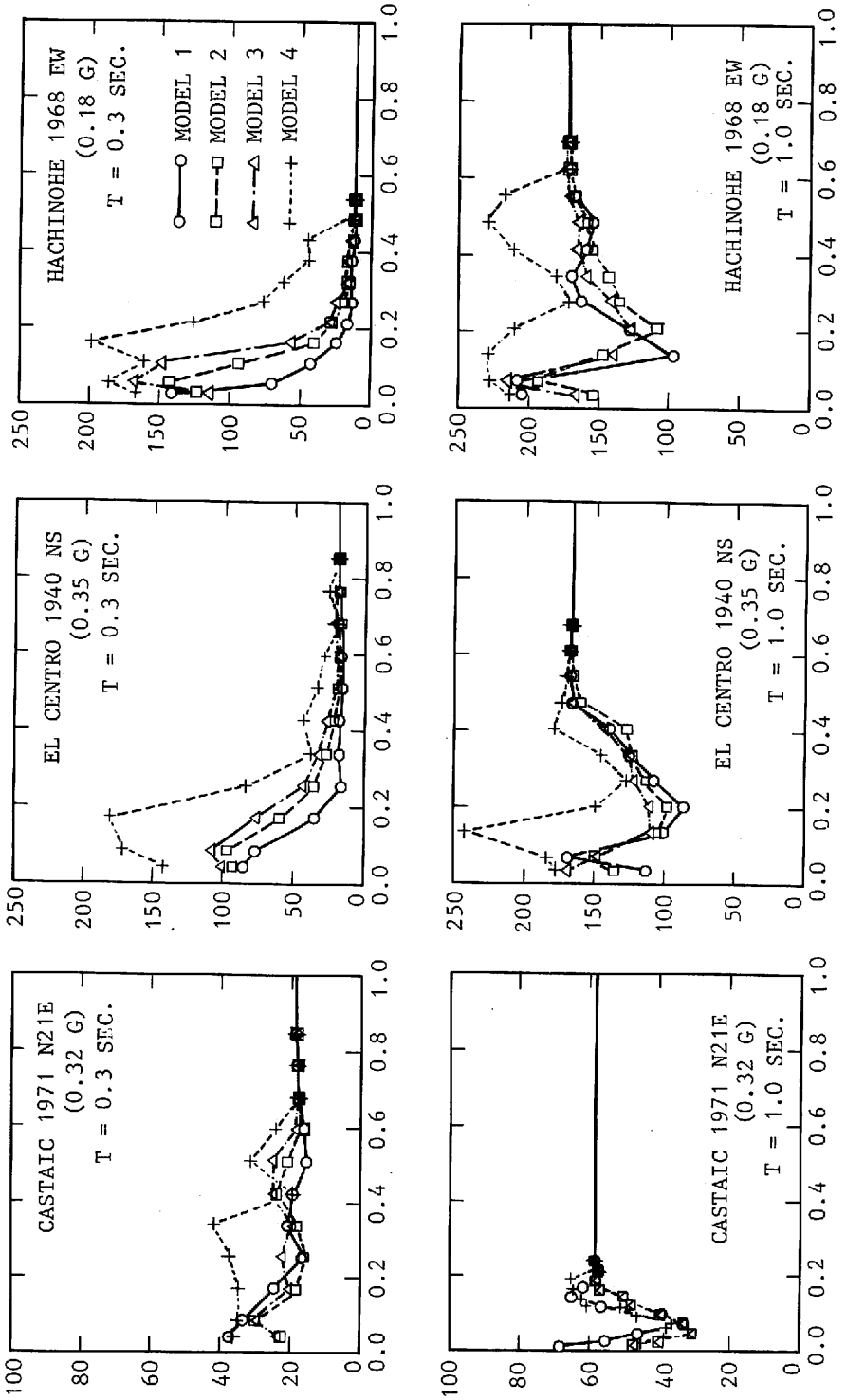

Fig. 11 Calculated Nonlinear Response for Various Hysteresis Models, Ground Motions and Initial Periods

the assumed shapes of the force-displacement relationship have more influence on energy dissipation if the displacement attained is large and the yield displacement is small. Comparisons of displacement response calculations with experimental results[15] have shown that hysteresis model 3 leads to satisfactory results for determining maximum displacement response of reinforced concrete structural models.

The data in Fig. 11 have been presented without modification to account for differences in intensity of the acceleration records. To permit direct comparisons among the displacement responses calculated for the three ground motions, a normalizing scheme was devised. Displacements and base shear strength coefficients were plotted as ratios of corresponding linear-response quantities calculated for a damping factor of 0.02. Displacement, DR, and strength, SR, ratios are defined below.

$$DR = D_n/D_s \tag{11}$$

$$SR = C_y/(A_s/g) \tag{12}$$

where,

D_s, A_s : displacement and acceleration responses for a linear oscillator with period T_0

D_n : displacement response for a nonlinear oscillator with initial period T_0

C_y : base shear strength coefficient (shear strength/weight)

g : acceleration of gravity

Figure 12 shows the relationship between normalized displacement and base shear strength. Each plot compares the response to the three ground motions for oscillators having the same initial period.

For oscillators with a 0.3-sec. initial period, the displacement ratio varies at different rates with the strength ratio, the rate depending on the ground motion. Because the plotted quantities have been normalized with respect to spectral response, it is assumed that the observed differences are caused by the differences in frequency content and, possibly, sequence rather than by differences in acceleration magnitudes. Displacement response for this case is seen to be insensitive to the

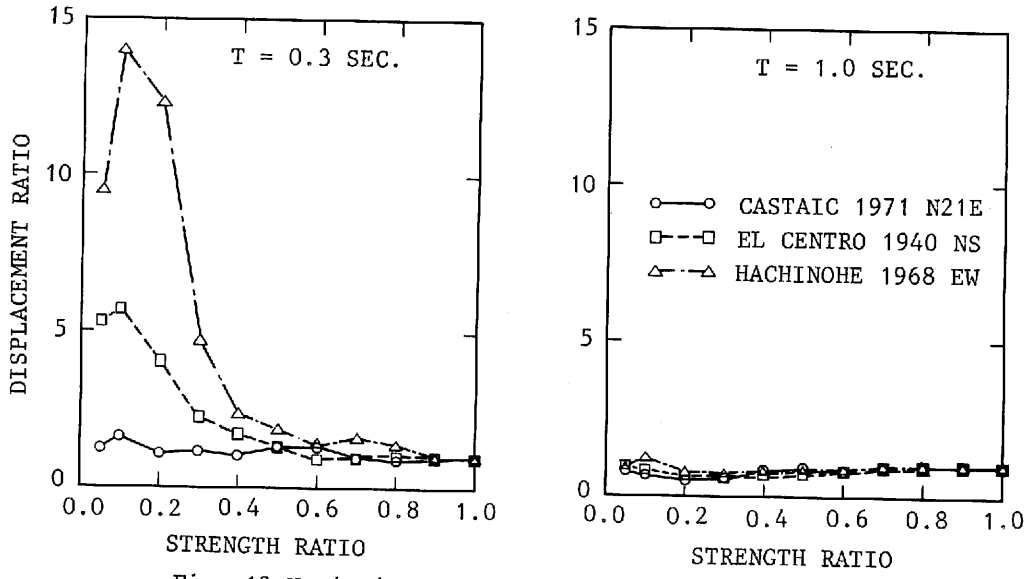

Fig. 12 Variation of Nonlinear Displacement Response with the Type of Ground Motion

strength ratio at strength ratios higher than approximately 0.5. Below that value, the displacement ratio appears to be quite sensitive to the ground motion attributed to a soft site (Hachinohe) and virtually insensitive to that for a hard site (Castaic) with the response for El Centro representing an intermediate case.

The displacement data in Fig. 12 refer to cases with base shear strength less than that required for linear response with a damping factor of 0.02. In every case up to a strength ratio of unity, calculated response extended beyond the break point in the assumed force-displacement relationship. As a result, the effective period increased and, in keeping with the assumed hysteresis model, the capability to dissipate energy or the area included in the largest hysteresis loop increased. These trends indicated by the calculated displacement ratios with the strength ratio and the type of ground motion may be rationalized with the help of the energy spectra (Fig. 5 through Fig. 7).

If the initial period of the oscillator is above the characteristic ground period TG, an increase in the effective period causes a small increase, if any, in the energy demand (Fig. 5 through Fig. 6). Under those conditions, the oscillator is able to dissipate the energy with little or even no further increase in displacement above that for linear response. If the initial period of the oscillator is below TG, and increase in the effective period is likely to result in an increase in the energy demand. The displacement response has to increase to dissipate the energy. Because the

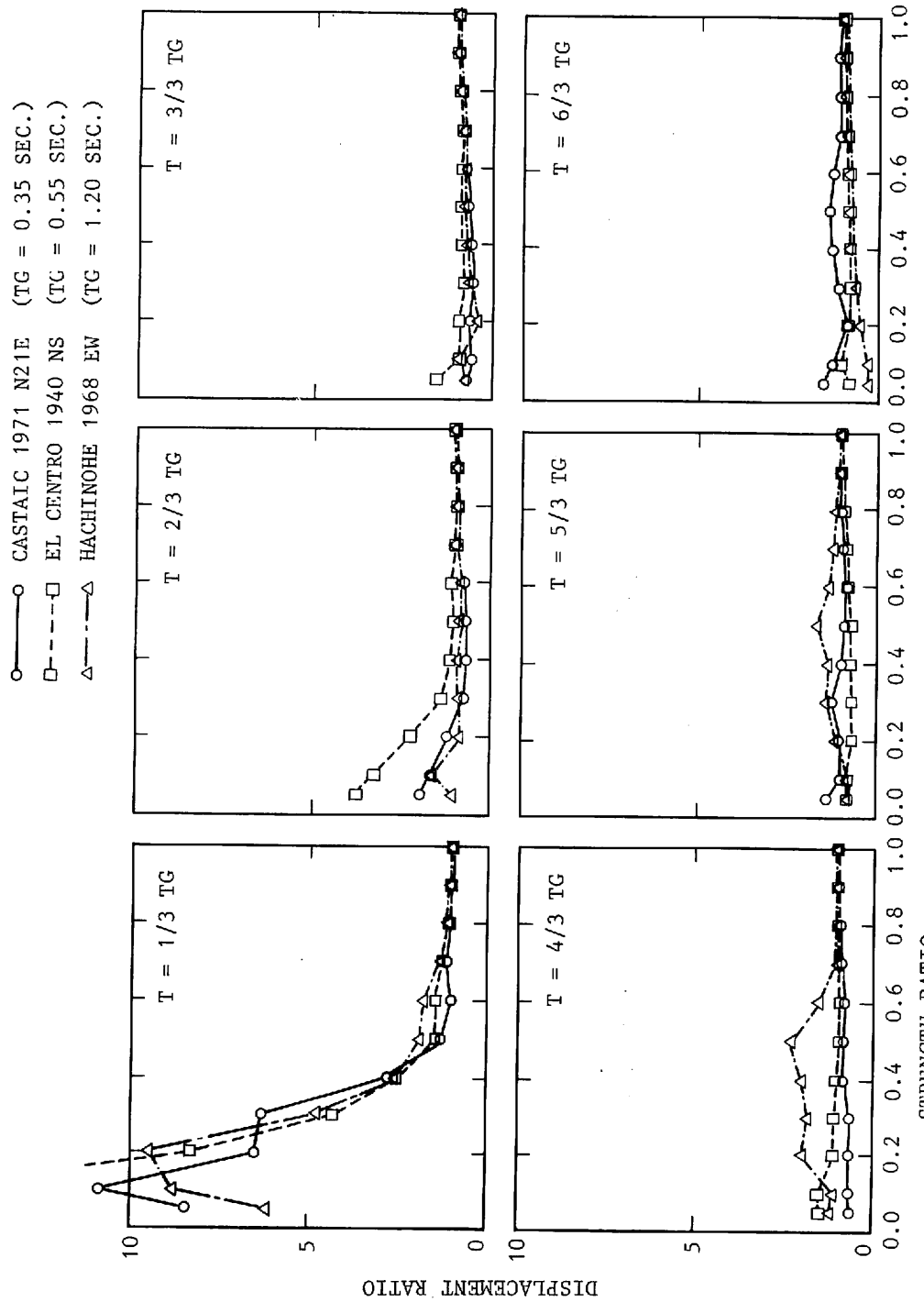

Fig. 13 Normalized Nonlinear Displacement Response

energy dissipated depends on the strength of the system as well as on displacement, the required increase in the displacement ratio is a function of the strength ratio; the increase in the displacement ratio decreases with increase in the strength ratio.

This rationalization suggests that the displacement ratios may be normalized to reflect the effect of the type of ground motion using the hypothesis that oscillators having similar period ratios, TR = T_0/TG (initial period/characteristic period for the ground motion), will have similar variations of the displacement ratio, DR, with the strength ratio, SR. Figure 13 tests this hypothesis.

Each one of the six plots in Fig. 13 compares variations of the displacement ratio with the strength ratio for equal values of the period ratio, TR, ranging from one-sixth to twice the period, TG, assumed to define site characteristics. In general, the data in the six plots indicate that the period ratio, TR, is appropriate for organizing the results of calculated displacements. There are some discordances. At TR = (4/3), data for Hachinohe tend to lie high. At TR = (2/3), the values for El Centro separate from the other two for low strength ratios. The calculated spectral response curves for Hachinohe (Fig. 7) show that it has very low response in the range 1.4 to 1.9 sec. Idealizing the displacement spectrum promises to improve consistency in Fig. 13.

A simple subjective procedure was used for determining the idealized

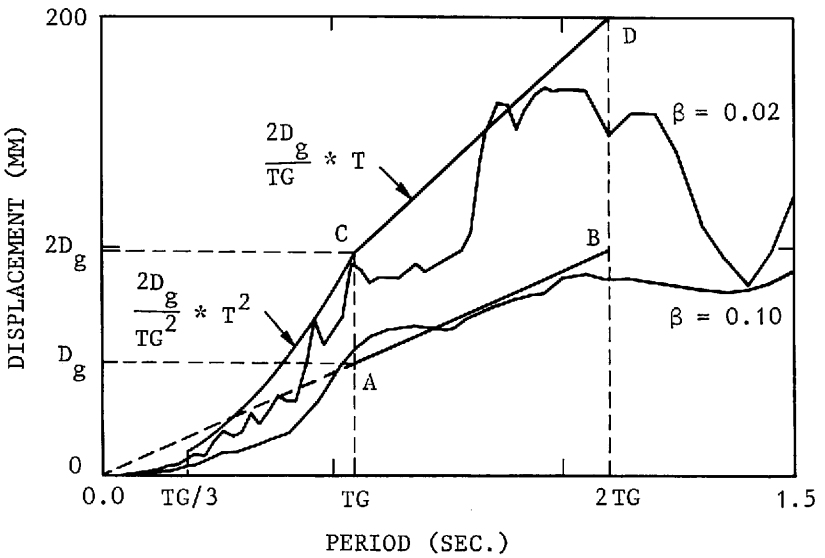

Fig. 14 Construction of the Idealized Displacement Response Spectrum for a Damping Factor of 0.02

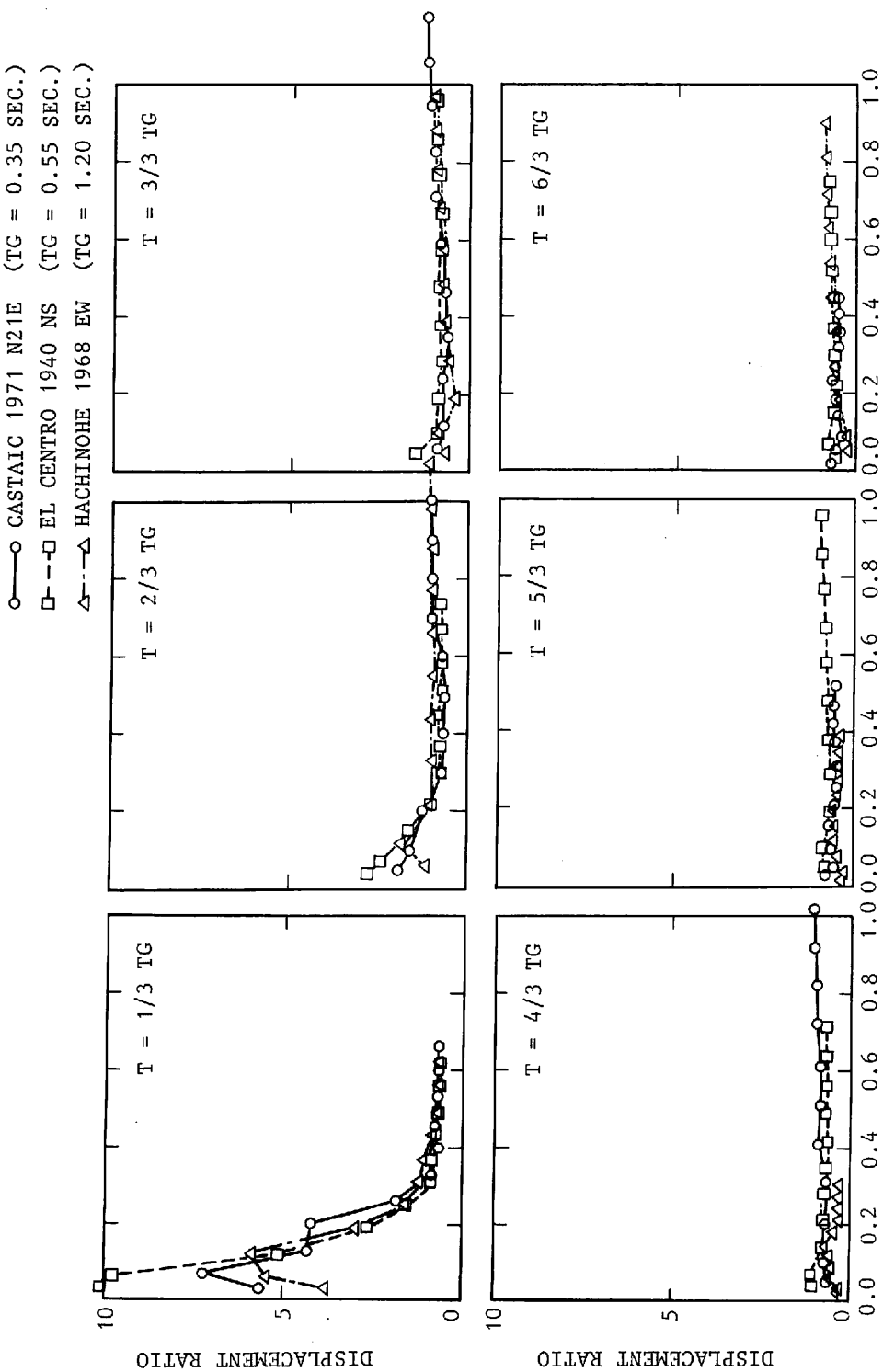

Fig. 15 Normalized Nonlinear Displacement Response Based on Idealized Displacement Response Spectra

response spectra by using the calculated response spectra for a damping factor of 0.02 as shown in Fig. 14. First, a line passing through the origin was chosen to provide a reasonable fit to the calculated curve between the periods TG and 2TG (Line AB in Fig. 14). It was assumed that the idealized spectrum for a damping factor of 0.02 would be line CD obtained by doubling the ordinates of line AB[16]. Idealized spectrum in the period range (TG/3) to TG was assumed to vary as the square of the period and have the ordinate $2D_g$ at TG.

Relationships between displacement and strength ratios based on idealized spectral response are shown in Fig. 15. The data plotted in Fig. 15 demonstrates that the parameters selected for normalizing displacement response are appropriate.

From the trends of the normalized data in Fig. 15, it may be concluded that:

(1) For TR + SR $\geq$ 1.0, the displacement ratio is likely to be approximately unity. Therefore, displacement response can be satisfactorily estimated using the spectral response value for a damping factor of 0.02.

(2) For TR + SR < 1.0, the displacement may be estimated by interpolating from the curves in Fig. 15 and 13.

These two complementary observations provide a basis for estimating drift of reinforced concrete buildings. It should be noted that the initial period considered in the paper corresponds to an intermediate value between the periods corresponding to uncracked and fully cracked section. For practical applications, the building period to be used in determining the period ratio, TR, may be assumed to be approximately $\sqrt{2}$ times the value for uncracked section or the value obtained from a simple relationship such as T = 0.1N, where N is the number of stories, for reinforced concrete frames. If the displaced shape of the building at the time of maximum expected drift can be estimated, distribution of deflection over the height of the building may be determined by procedures described in References 17) or 18).

6. SUMMARY

In order to investigate the possibility of developing a simple procedure for determining seismic drift of reinforced concrete buildings, a

parametric study was made using single-degree-of-freedom oscillators with hysteresis properties simulating the behavior of reinforced concrete systems. The main variables considered were initial stiffness, strength, and type of ground motion. Scope of the variable combinations included in the study is summarized by Fig. 11. The two initial periods, 0.3 and 1.0 sec., reflect the stiffnesses. The three ground motions selected are assumed to be representative of motions for hard, medium, and soft ground. Nonlinear response was calculated for a series of oscillators of increasing strength in each case. The straight horizontal lines in each figure represent maximum linear response for the initial period of the oscillator at a damping factor of 0.02.

Values of strength and calculated displacement were normalized by expressing them as strength and displacement ratios or as ratios of the pertinent linear-response (damping factor = 0.02) values defined by Eq. (11) and (12). Trends of displacement ratios with strength ratios (Fig. 12) indicated that the period ratio, or the ratio of the initial period of oscillator to characteristic period of the ground motion TG determined using the energy spectrum, could be used to organize the data for the types of ground motion considered. Plots of displacement vs strength ratio organized accordingly (Fig. 15) demonstrated that the nonlinear-response displacement was essentially the same as the displacement obtained from a linear-response calculation with a damping factor of 0.02, provided the sum of the strength and period ratios was not less than one. If the sum is less than one, the displacement may be estimated by interpolation from the data in Fig. 15. These two generalizations provide the basis of a simple procedure for estimating drift. As a minimum, they will help identify whether the drift estimate can be accomplished using a linear-response spectrum or whether more detailed modeling and calculations are required.

7. ACKNOWLEDGEMENTS

The first writer participated in this study while he was a visiting scholar at the University of Illinois in connection with the U.S.-Japan Cooperative Research Program Utilizing Large-Scale Testing Facilities.

The first writer gratefully acknowledges Professor Watabe, Tokyo Metropolitan University, and Building Constructors Society about their efforts for visiting.

D. Bever is thanked for typing this report. The CDC Cyber 175 computer system of Computing Services Office and the DEC LSI/23 computer system of

the Civil Engineering Department of University of Illinois were used for the computations. Support was provided by NSF grant CEE-81-14977.

8. REFERENCES

1) Sheth, R.M., "Effect of Inelastic Action on the Response of Simple Structures to Earthquake Motions", M.S. Thesis, University of Illinois, Department of Civil Engineering, 1959.
2) Veletsos, A.S. and N.M. Newmark, "Effect of Inelastic Behavior on the Response of Systems", Proceedings of the Second World Conference on Earthquake Engineering, Tokyo and Kyoto, Vol. II, pp.895-912, 1960.
3) Otani, S., "Hysteresis Models of Reinforced Concrete for Earthquake Response Analysis", Journal of the Faculty of Engineering (B), University of Tokyo, Tokyo, Vol. 36, No. 2, pp.125-159, 1981.
4) Kato, B. and H. Akiyama, "Energy Input and Damages in Structures Subjected to Severe Earthquakes (In Japanese)", Transaction of the Architectural Institute of Japan, Tokyo, Vol. 235, pp.9-18, 1975.
5) Housner, G.W., "Limit Design of Structures to Resist Earthquakes", Proceedings of the First World Conference on Earthquake Engineering, California, pp.5-1 to 5-13, 1956.
6) Akiyama, H., "Aseismic Ultimate Design of Building Structures (In Japanese)", Tokyo University Press, Tokyo, 1980.
7) Suzuki, T. and T. Takeda, "The Relationship Between the Strength and Plastic Deformation of Buildings Based on Energy Concept (In Japanese)", Proceedings Kanto District Symposium, Architectural Institute of Japan, Tokyo, pp.89-92, 1981.
8) Trifunac, M.D., F.E. Udwadia and A.G. Brady, "Analysis of Errors in Digitized Strong-Motion Accelerograms", Bulletin of Seismological Society of America, Vol. 63, No. 1, pp.157-187, February 1973.
9) Hodder, S.B., "Computer Processing of New Zealand Strong-Motion Accelerograms", Proceedings of the Third South Pacific Regional Conference on Earthquake Engineering, New Zealand, Vol. I, pp.36-53, 1983.
10) Sunder, S.S. and J.J. Connor, "A New Procedure for Processing Strong-Motion Earthquake Signals", Bulletin of the Seismological Society of America, Vol. 72, No. 2, pp.643-661, April 1982.
11) Clough, R.W. and S.B. Johnston, "Effect of Stiffness Degradation on Earthquake Ductility Requirements", Proceedings of the Second Japan Earthquake Engineering Symposium, pp.227-232, 1966.
12) Takeda, T., M.A. Sozen and N.N. Nelson, "Reinforced Concrete Response to Simulated Earthquakes", Journal of Structural Division, ASCE, Vol. 96, No. ST12, pp.2557-2573, 1970.

13) Jacobsen, L.S., "Damping in Composite Structures", Proceedings of the Second World Conference on Earthquake Engineering, Tokyo and Kyoto, Vol. II, pp.1029-1044, 1960.

14) Newmark, N.M., "A Method of Computation for Structural Dynamics", Journal of Structural Division, ASCE, Vol. 85, No. ST3, pp.67-94, 1959.

15) Saiidi, M. and M.A. Sozen, "Simple and Complex Models for Nonlinear Seismic Response of Reinforced Concrete Structures", Structural Research Series No. 465, Department of Civil Engineering, University of Illinois, August 1979.

16) Shibata, A. and M.A. Sozen, "Substitute-Structure Method for Seismic Design in R/C", Journal of the Structural Division, ASCE, Vol. 102, No. ST1, pp.1-18, January 1976.

17) Okamoto, S., S. Nakata, Y. Kitagawa, M. Yoshimura and T. Kaminosono, "A Progress Report on the Full-Scale Seismic Experiment of a Seven-Story Reinforced Concrete Building - Part of the US-Japan Cooperative Program", Building Research Institute Research Paper, No. 94, Ministry of Construction, Japan, 1982.

18) Rothe, D.H. and M.A. Sozen, "A SDOF Model to Study Nonlinear Dynamic Response of Large- and Small-Scale R/C Test Structures", Civil Engineering Studies, Structural Engineering Research Series No. 512, University of Illinois, Urbana, 1983.

UDC 624.920.427 :534.014

鉄筋コンクリート構造物の地震時変形

技術研究所　島 崎 和 司
イリノイ大学・教授　M. A. ソーゼン

キーワード：鉄筋コンクリート，地震応答，地震波，非線形システム，応答スペクトル，エネルギースペクトル，耐震設計，1質点系

要　　旨

適当な履歴モデルによる1質点系に対するパラメトリックな非線形解析によって，鉄筋コンクリート構造物の非線形変位応答を検討した。この研究において考慮した主な因子は，強度，剛性，および地震波の特性である。結論として，上記3種の因子によって定義される無次限量をパラメーターとして，変位応答が線形応答解析を用いて充分な精度で求められるか否かを決定出来る事を示した。

目　　次